Mechanical and degradation properties of zinc adopted magnesium alloys for biomedical application

IOP Conf. Series: Materials Science and Engineering **602** (2019) 012094 doi:10.1088/1757-899X/602/1/012094

Mechanical and degradation properties of zinc adopted magnesium alloys for biomedical application

I P Nanda[1], M H Hassim[2], M H Idris[2], M H Jahare[2], S S Abdulmalik[2], and A Arafat[3]

[1]Department of Mechanical Engineering, Universitas Andalas, Padang, Indonesia
[2]School of Mechanical Engineering, Universiti Teknologi Malaysia, Johor, Malaysia
[3]Department of Mechanical Engineering, Universitas Negeri Padang, Padang, Indonesia.

E-mail: arafat@ft.unp.ac.id

Abstract. The demand for short-term degradable implant in bone fixation applications is growing steadily due to the aging population worldwide. Degradable implants have the advantage that the second surgery for implant removal is not required. Magnesium is one of the best candidates because it is biodegradable, physiologically compatible and even stimulates bone reconstruction. However, the high degradation rate of pure magnesium in human body fluids may prevent its wider application. In this study, Zinc (Zn) was added in magnesium (Mg) to improve its properties. The effects of five different weight percentage of Zinc (2%, 4%, 6%, 8%, 10%) were investigated. The microstructure and mechanical properties evolution of the alloys were characterized and evaluated using optical microscopy, Scanning Electron Microscope (SEM), tensile test and Vickers hardness test, while degradation behavior was examined using electrochemical corrosion test. The binary Mg-Zn cast alloy with 6 wt. % zinc content (labeled as Mg-6Zn) shows optimum mechanical strength with slowest degradation rate.
Keywords - Mg-Zn alloys; biomedical application; mechanical properties; biodegradation

1. Introduction

Biomaterials used as implants in the body have been emerging over the past half of century, and currently a great number of implants available throughout all medical application such as orthopedic surgery, general surgery, maxillofacial surgery, cardiology, gynecology, and urology. Implantation of artificial bone fixation requires it to stay in the body permanently, while certain implication only requires implant support for a short period. When a permanent implant is used for a temporary application, additional surgeries are required to remove these devices after the healing process. Thus, the removal process increases the patient grim and cost of health care.

On the other hand, biodegradable implants offer advantages over metal analogs in term of zero implant removal, zero revision surgery, and minimum radiological imaging, as they dissolve in a period [1]**.** It provides resultant high strength while allowing osseointegration and replacement by the host tissue. The biodegradable implant also eliminates the complications associated with the long-term presence of implants in the body.

The material for biodegradable implants is essential to have few characteristics such as biocompatible, bioabsorbable, secure initial fixation strength and promote osseointegration [2]. Magnesium is a suitable candidate for this requirement. Pure Magnesium can be metabolized by the body system and is the fourth highest element present in the human body. Normal adult consumed about 300 to 400 mg of magnesium daily, and Mg2+ excessive is not toxic and ejaculated through the urinary system [3]**.** Magnesium also has a value of elastic modulus, compressive yield strength and density close to the natural bone [4]**.** In vitro cell test on pure magnesium showed positive cell proliferation and viability with no sign of growth inhibition [5]**.** However, the critical issue for pure Mg is due to the relatively very susceptible to degradation, inadequate strength, the release of hydrogen gas and a relatively high degradation rate in the human body [6]. Rapid degradation rates consequently disturb bone ingrowth performance, thus making healing problematic. For a better effect of these materials in the human body, their degradation behavior needs to be altered, and the interactions between the degradation product and the biological environment need to be explored.

Alloying with other biocompatible materials is of special interest in the biomedical application. Zn is one of important elements in the body system and has a positive record in biomedical applications. It was reported that zinc could improve the strength of magnesium alloy through increase age hardening response, produce intermetallic compounds, refine grain size and improve castability [7]. The addition of Zn can improve both tensile strength and ductility of the alloys as well as reduces the degradation rate by slowing the rate of anodic dissolution [8].

The degradation resistance of alloying-element in Mg alloys is not widely reported and therefore not well established. The toughness of pure magnesium is greater than that of ceramics. However it degrades rapidly in the human body system, losing strength before tissue healing. To maintain the mechanical integrity, and biocompatibility, sufficient alloying content is essential. Thus, the interaction between microstructure, phase transformation and degradation properties of the alloying composition must be extensively investigated. This study, therefore, contributes to clarifying the correlation between alloying and degradation, which plays an important role in an efficient alloy design for accomplishing desired benefits.

2. Material and method

Mg-Zn alloys were prepared by melting pure 99.99 wt.% Mg (Figure 1(a)) and pure 99.99 wt% Zn (Figure 1(b)) in an induction furnace (Figure 2(a)). A graphite crucible was used, and the metal was melted under a flowing argon atmosphere to prevent ignition and oxidation of the molten metal. Pure Zn was added into crucible after magnesium metal was melted at about 650^{o}C. The temperature was maintained at 750^{o}C for about 15 minutes while vigorously stirred 7-9 times. The molten Mg-Zn alloy was then poured into a preheated steel mold (Figure 2 (b)).

Figure 1. Pure magnesium and pure zinc

Figure 2. Induction furnace and steel mold

The surface morphology, microstructure, and phases distribution for produced Mg-Zn alloys were observed using an Olympus BX-60 optical microscope and Philips XL-40 scanning electron microscope equipped with energy dispersive spectroscopy (EDS. Before the analysis, the samples were polished up to mirror finish by using a polishing cloth and alumina suspension.

Vickers microhardness test was performed on alloys surface to reflect the ability to resist plastic deformation. The tests were performed using Matsuzawa DVK-2 microhardness testing machine conforming to the ASTM-E98-82 standard. Before the test, the samples were ground up to 1200 grit SiC paper finish and then cleaned with acetone and hot air. Data concluded in this study were an average value of 5 measurements at a different location.

The tensile strength values of the alloys were tested with a tensile speed of 1 mm/min using an Instron universal testing machine. The tests were conducted according to ASTM-A370. The specimens were prepared from the as-cast Mg-Zn alloy with a gauge length of 25mm and thickness of 10mm. The elongation was determined using extensometer. A minimum of 4 separate tests was performed for each alloy.

To explain the mechanistic aspects that determine the ultimate degradation rates realized, the principal corrosion test method used in this study is potentiodynamic polarisation. The corrosion test was carried out in the solution of simulated body fluid at the temperature of 37 ± 1 ^{o}C using an advanced electrochemical system of potentiostat (Parstat-2263), with three electrode cells of saturated calomel electrode (SCE) as a reference electrode, graphite electrode as counter electrodes, and the sample as the working electrode. The surface area of the sample exposed to the electrolyte was 1 cm^2. The polarization in the anodic direction proceeded at a scan rate of 0.9 mV/s. The potentiodynamic curves of pure Mg and Mg-Zn alloys were analyzed by Tafel extrapolation method, and the values of corrosion potential (E_{corr}) and corrosion current density (i_{corr}) have been obtained. Degradation rate has been calculated using the values of E_{corr} and i_{corr}. Three replicates were conducted for each group of samples.

3. Result and discussion

3.1. Effect of Zn alloying on the microstructure

The chemical compound of the specimens was examined by Energy Dispersive Spectrometer (EDS) connected to Scanning Electron Microscopy (SEM), has appeared in Table 4.1.

Table 1. The chemical composition of the Mg-Zn alloys in wt. %

Sample	Code	Zn	Mg
1	Mg-2Zn	1.62	98.38
2	Mg-4Zn	4.03	95.97
3	Mg-6Zn	6.33	93.67
4	Mg-8Zn	8.46	91.54
5	Mg-10Zn	9.65	90.35

Figure 3 shows the optical microstructures of pure Mg and as cast Mg–Zn alloys. All materials show nearly equiaxed grain structure. In Figure 3b to f, it can be observed that after Zn addition, eutectics form mainly along the grain boundaries of Mg were present, and the width of eutectics along grain boundary becomes clearer as the content of zinc increases. According to the Mg-Zn phase diagram [9], the eutectics were predominantly composed of Mg_2Zn_{11} and $MgZn_2$. The development of $MgZn_2$ over the equilibrium phase Mg_2Zn_{11} was expected to non-balance solidifying conditions experienced by the alloy during fast cooling in a ferrous mold under atmospheric environment [10]. Moreover, the grain boundaries are portrayed by an intermittent conveyance of small precipitates.

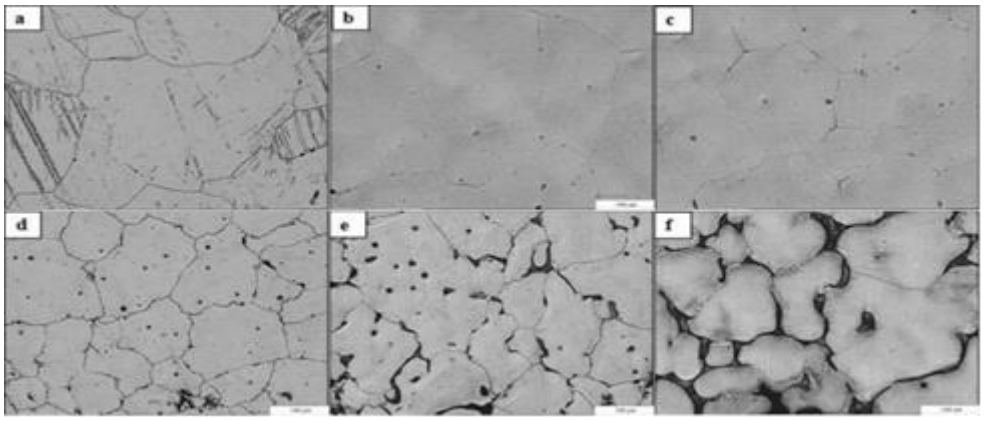

Figure 3. Optical microstructure pure Mg and Mg-Zn alloys (a) pure Mg, (b) Mg-2Zn, (c) Mg-4Zn, (d) Mg-6Zn, (e) Mg-8Zn, (f) Mg-10Zn

3.2. Effect of Zn alloying on mechanical properties

Vickers hardness tester measures the resistance of a material to indentation. During testing, the indenter is pushed into the sample surface normally. The ASTM-E98-82 standard was followed for testing the hardness of the benchmark components. The hardness of specimens was measured five times in different places to reduce the measurement error. The hardness based on wt.% alloy composition of all samples tested in this study appears in Figure 4. It is observed that the hardness of Mg-Zn alloys is improved essentially because of alloying augmentations (for 2, 4 and 6 wt.% alloying), and then slightly drop at Mg-8Zn and Mg-10Zn alloys. Most outcomes represent a general pattern that increasing total alloying loading in Mg prompts higher hardness, in a moderately monotonic manner. Slight drop in hardness value for 8 and 10 wt.% alloying may be ascribed by the development of the secondary phases on these alloys Mg-8Zn, and Mg-10Zn. Since the maximum solubility of zinc in magnesium is 6.2 wt.% and as previously reported that the excess Zinc will interact with Mg and form abundant of Mg and Zn containing phases in the matrix and grain boundary [11]. These phases isolate the matrix and increase the number of crack sources. Consequently, disturb the mechanical properties improvement.

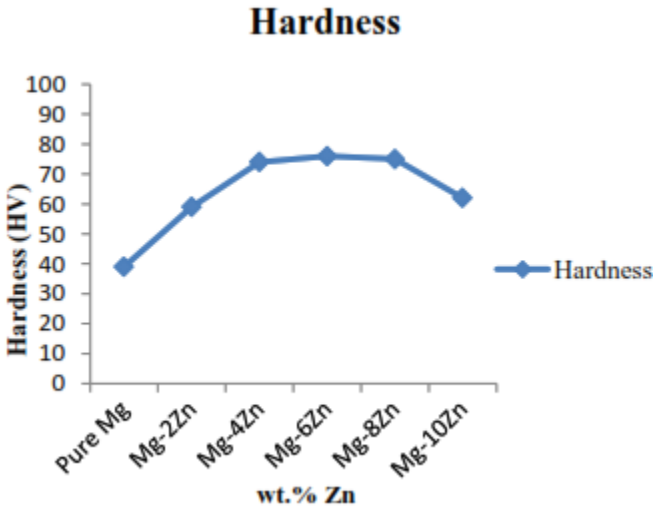

Figure 4. Vickers microhardness value of Mg-Zn alloys based on Zn wt.%

The tensile strength of the alloy based on Zn wt.% is shown in figure 4. It is also observed that the tensile strength value increases until 6 wt.% of Zn while it drops when reaching 8 and 10 wt.% of Zn. Also, Table 2 summarized the value of tensile strength, yield strength and elastic modulus of the Mg-Zn alloys. While the pattern of tensile strength and yield strength follow a similar trend as the hardness graph, the elastic modulus value shows an irregular pattern. These phenomena of the may be attributed to the formation of secondary phase by the excessive presence of Zn. Zn reacts with magnesium and progress toward becoming wellsprings in the matrix and the grain boundary, hence, the elasticity of the alloy decrease [11].

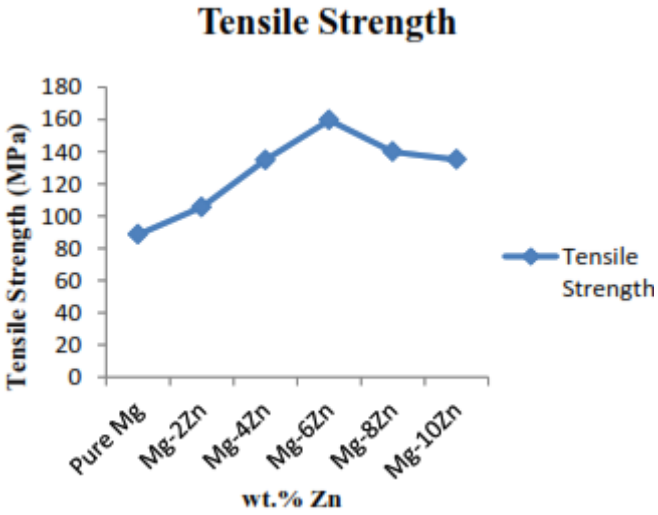

Figure 5. Tensile strength value of Mg-Zn alloys based on Zn wt.%

Table 2. The Tensile strength, Yield, and Elastic Modulus value of Mg-Zn alloys

Sample	Tensile Strength (MPa)	Yield strength (MPa)	Modulus (GPa)
Pure Mg	88.5	27.5	37.5
Mg-2Zn	105.57	54.19	35.94
Mg-4Zn	134.82	65.61	29.93
Mg-6Zn	159.57	128.8	48.66
Mg-8Zn	139.84	89.98	41.55
Mg-10Zn	135.12	83.43	33.29

Alloying Mg with Zn will lead to grain refinement and development of the second phase along the grain boundary and matrix [12]. According to Xiaobo Zhang et al., non-basal dislocation slip, as well as basal dislocation slip, were actuated in fine grain Mg alloys as a result of the grain boundary compatibility impact and their HCP crystal structure [13]. It implies that for the single-crystal Mg, at ambient air environment the disfigurement mechanism of the material is dominated by the basal dislocation slips. Nonetheless, due to neighboring grains restraint, the circumstance in the polycrystalline Mg alloys is unique. The occurrence of basal dislocation slip in polycrystal can lead to strain incompatibility at grain boundaries. For Mg alloys, the grain boundaries are sufficiently solid thus extra stress emerges to keep up strain compatibility at grain boundaries. This compatibility stress promotes to the initiation of non-basal dislocations slip. In this manner refinement of grains because of Zn integration can constrain the occurrence of dislocations and confine the movement of the non-basal dislocations slip mechanisms which improve the mechanical performance of the alloy [14].

Moreover, based on the Mg-Zn binary phase diagram, in the stable state, the highest possible solubility of Zn in Mg is up to 1.6 wt.% at room temperature. Subsequently, the Zn element dissolved into α-Mg to some amount [15] and developed intermetallic MgZn phases. Subsequently, with expanding Zn content from 2wt.% to 6wt.% in Mg-Zn alloy, similar with grain strengthening, solid solution strengthening and second phase strengthening enhance the mechanical behavior of Mg-Zn alloys. On the other hand, the grains are more refined, and a total of intermetallic phases in Mg-8Zn and Mg-10Zn alloys is greater than lower Zn alloys. Expanding the total of intermetallic phases and precipitating of these Mg-Zn phases along the grain boundaries can viably fortify the alloy grain boundaries [13] which increase the strength of-of the Mg-Zn alloys compare to pure Mg. Table 2 likewise demonstrates that by adding more than six wt.% Zn tensile strength of the Mg-Zn alloy decreased. It was specified by the previous researcher that the precipitated second phase could impressively enhance the hardness while reducing the ductility of the alloys [16]. In another word, the second phase may expand the dislocation density.

3.3. Effect of Zn alloying on degradation performance

Potentiodynamic polarization curves provide useful information on the degradation behavior and degradation rate. The potentiodynamic polarization curves measured in simulated body fluid solution for Mg-Zn alloys samples are displayed in Figure 6. The corrosion potential (E_{corr}) and the corrosion current densities (i_{corr}) derived from the polarization curves by using Tafel extrapolation method are mentioned in Table 3. Electrochemical tests showed that alloying is a promising way to improve the degradation properties of Mg. As expected, the polarization curves for all Mg-Zn alloys indicate lower current density and more positive potential, while pure Mg exhibits the most negative corrosion potential (−2.027 V). The corrosion potential of the alloy increases as the content of Zn increases. This indicates the improvement in degradation resistance of the Mg by alloying. The enhanced degradation properties are attributed due to the formation of the MgZn phase in the alloy matrix, which directly proportional to the increase of Zn content [12]. Generally, this MgZn phase protects by acting as a barrier against electrons and ions diffusion, thus reducing the electrochemical reactions of alloy and

electrolyte. For this reason, Mg-6Zn samples offer better degradation resistance properties compared to Mg-2Zn and Mg-4Zn specimens.

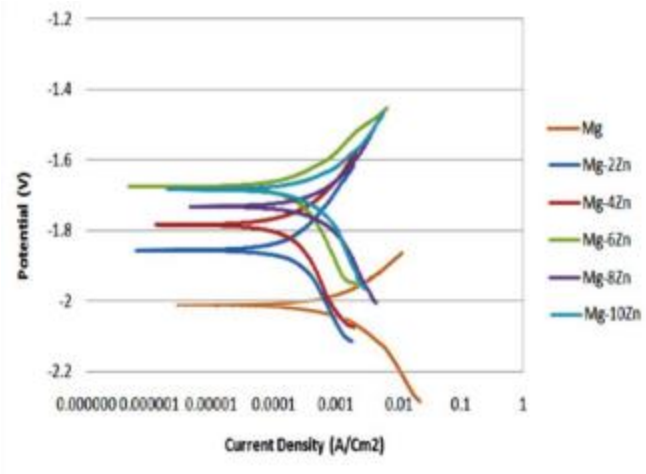

Figure 6. Electrochemical polarization curves of Mg-Zn alloys under investigation

However, the E_{corr} decrease after Zn content exceeds 6 wt.%. It was reported that the increase in Zn content over 6 wt.% would promote other intermetallic phase formation in the alloys [12]. These phases created a ceaseless network structure, prompting to the development of more anode-cathode sites. Hence, more galvanic degradation would occur, leading in a high degradation rate. Thus, it can be concluded that the degradation performance of Mg-8Zn and Mg-10Zn alloys are induced by the galvanic couple reaction, which accelerated the dissolution of the α-Mg matrix, and directly contributed to increment of degradation rate.

Table 3. Potentiodynamic polarization curveparameters derived by the Tafel extrapolation

Specimen	E_{corr} (V)	i_{corr} (μA)	Corrosion rate (mmpy)
Pure Mg	–2.027	309	7.06
Mg–2Zn	–1.860	210	4.8
Mg-4Zn	–1.781	187.5	4.28
Mg–6Zn	–1.675	122	2.78
Mg–8Zn	–1.761	178.4	4.07
Mg–10Zn	–1.740	135	3.08

4. Conclusion

According to the objective of the experiment, analyzes that have been performed, and interpretation of the results, it can be concluded that:

i. Mechanical properties of the Mg improved as the Zn content increased from 2 to 6wt%. Further increase of Zn content until 10 wt.% resulted in a considerable drop in mechanical performance.
ii. Zn addition up to 6wt.% provided 3 times better degradation resistance when compared with pure Mg due to the formation of the MgZn phase. The present of $Mg_{51}Zn_{20}$ phase in Zn content more than 6wt.% leads to rapid degradation rate.

5. Acknowledgment
Authors highly appreciate the great support and encouragement from all who contribute in this work. This work was supported by the Ministry of Higher Education (MOHE), Malaysia under the fundamental research grant scheme (Grant no: FRGS/1/2015/TK03/UTM/01/3).

References
[1] H. R. Bakhsheshi-Rad, M. R. Abdul-Kadir, M. H. Idris, and S. Farahany, "Relationship between the corrosion behavior and the thermal characteristics and microstructure of Mg-0.5Ca-xZn alloys," *Corros. Sci.*, vol. 64, pp. 184–197, 2012.
[2] M. Moravej and D. Mantovani, "Biodegradable metals for cardiovascular stent application. Interests and new opportunities," *Int. J. Mol. Sci.*, vol. 12, no. 7, pp. 4250–4270, 2011.
[3] H. R. Bakhsheshi-Rad, M. H. Idris, M. R. A. Kadir, and M. Daroonparvar, "Effect of fluoride treatment on corrosion behavior of Mg-Ca binary alloy for implant application," *Trans. Nonferrous Met. Soc. China (English Ed.*, vol. 23, no. 3, pp. 699– 710, 2013.
[4] H. R. B. Rad, M. H. Idris, M. R. A. Kadir, and S. Farahany, "Microstructure analysis and corrosion behavior of biodegradable Mg-Ca implant alloys," *Mater. Des.*, vol. 33, no. 1, pp. 88–97, 2012.
[5] S. Keim, J. G. Brunner, B. Fabry, and S. Virtanen, "Control of magnesium corrosion and biocompatibility with biomimetic coatings," *J. Biomed. Mater. Res. - Part B Appl. Biomater.*, vol. 96 B, no. 1, pp. 84–90, 2011.
[6] M. P. Sealy and Y. B. Guo, "Fabrication and Characterization of Surface Texture for Bone Ingrowth by Sequential Laser Peening Biodegradable Orthopedic Magnesium-Calcium Implants," *J. Med. Device.*, vol. 5, no. 1, p. 011003, 2011.
[7] S. Farahany, H. R. Bakhsheshi-Rad, M. H. Idris, M. R. Abdul Kadir, A. F. Lotfabadi, and A. Ourdjini, "In-situ thermal analysis and macroscopical characterization of Mg-xCa and Mg-0.5Ca-xZn alloy systems," *Thermochim. Acta*, vol. 527, pp. 180–189, 2012.
[8] K. B. Devi, B. Lee, A. Roy, P. N. Kumta, and M. Roy, "Effect of zinc oxide doping on in vitro degradation of magnesium silicate bioceramics," *Mater. Lett.*, vol. 207, pp. 100– 103, 2017.
[9] T. Prosek, A. Nazarov, U. Bexell, D. Thierry, and J. Serak, "Corrosion mechanism of model zinc-magnesium alloys in atmospheric conditions," *Corros. Sci.*, vol. 50, no. 8, pp. 2216–2231, 2008.
[10] Y. qi Wang, G. Kong, C. shan Che, T. Yu Weng, and Z. wen Sun, "Corrosion behavior of Zn-Mg alloys in saturated Ca(OH)2solution," *Corros. Sci.*, vol. 136, no. November 2016, pp. 374–385, 2018.
[11] Y. Dongsong and Z. Erlin, "Effect of Zn content on microstructure, mechanical properties and fracture behavior of Mg-Mn alloy," no. February, pp. 43–47, 2009.
[12] A. Lotfabadi, M. Idris, a L. I. Ourdjini, M. Abdul Kadir, S. Farahany, and H. Bakhsheshi- Rad, "Thermal characteristics and corrosion behavior of Mg- xZn alloys for biomedical applications.," *Bull. Mater. Sci.*, vol. 36, no. 6, pp. 1103–1113, 2013.
[13] X. Zhang, Z. Wang, G. Yuan, and Y. Xue, "Improvement of mechanical properties and corrosion resistance of biodegradable Mg-Nd-Zn-Zr alloys by double extrusion," *Mater. Sci. Eng. B Solid-State Mater. Adv. Technol.*, vol. 177, no. 13, pp. 1113–1119, 2012.
[14] B. Q. Shi, R. S. Chen, and W. Ke, "Influence of grain size on the tensile ductility and deformation modes of rolled Mg-1.02 wt.% Zn alloy," *J. Magnes. Alloy.*, vol. 1, no. 3, pp. 210–216, 2013.
[15] H. Somekawa, Y. Osawa, and T. Mukai, "Effect of solid-solution strengthening on fracture toughness in extruded Mg-Zn alloys," *Scr. Mater.*, vol. 55, no. 7, pp. 593–596, 2006.
[16] D. song YIN, E. lin ZHANG, and S. Yan ZENG, "Effect of Zn on the mechanical property and corrosion property of extruded Mg-Zn-Mn alloy," *Trans. Nonferrous Met. Soc. China (English Ed.*, vol. 18, no. 4, pp. 763–768, 2008.